

A FLIGHT EXPERIMENT TO MEASURE RAREFIED-FLOW AERODYNAMICS

Robert C. Blanchard*
NASA Langley Research Center
Hampton, Virginia

Abstract

A flight experiment to measure rarefied-flow aerodynamics of a blunt lifting body is being developed by NASA. This experiment, called the Rarefied-Flow Aerodynamic Measurement Experiment (RAME), is part of the Aeroassist Flight Experiment (AFE) mission, which is a Pathfinder design tool for aeroassisted orbital transfer vehicles. The RAME will use flight measurements from accelerometers, rate gyros, and pressure transducers, combined with knowledge of AFE in-flight mass properties and trajectory, to infer aerodynamic forces and moments in the rarefied-flow environment, including transition into the hypersonic continuum regime. Preflight estimates of the aerodynamic measurements are based upon environment models, existing computer simulations, and ground test results. Planned maneuvers at several altitudes will provide a first-time opportunity to examine gas-surface accommodation effects on aerodynamic coefficients in an environment of changing atmospheric composition. A description is given of the RAME equipment design.

Nomenclature

A standardized aerodynamic acceleration, a/C
 a acceleration
 C aerodynamic force coefficient
 \bar{C} normalized rarefied-flow aerodynamic coefficient
 g gravitational acceleration at sea level
 Kn Knudsen number, ratio of mean free path to vehicle reference length (ref. = 14 ft)
 M mass
 p pressure
 S area
 s molecular speed ratio
 T temperature
 V velocity
 α angle of attack
 β angle of sideslip

*Senior Research Engineer,
 Aerothermodynamics Branch, Space
 Systems Division

ρ density
 μ 10^{-6} g, where g is the gravitational acceleration at sea level
 ω bridging parameter

Abbreviations

AFE Aeroassist Flight Experiment
 AOTV aeroassisted orbital transfer vehicle
 c.g. center of gravity
 DFE data format electronics
 DSMC direct simulation Monte Carlo
 GEO geosynchronous orbit
 HiRAP High Resolution Accelerometer Package
 LINS Laser Inertial Navigation System
 RAME Rarefied-Flow Aerodynamic Measurement Experiment
 RMS remote manipulator system
 SRM solid rocket motor
 TDRSS Tracking and Data Relay Satellite System
 3D three dimensional

Subscripts

A axial force
 C continuum
 D drag
 F free molecule flow
 L lift
 m pitching moment
 N normal force
 stag stagnation
 Y side force
 w wall
 ∞ free stream
 1976 refers to 1976 standard atmosphere

Introduction

Designers have known for some time that a vehicle's kinetic energy can be exchanged with atmospheric thermal energy for a significant payload enhancement for certain types of orbit transfer.¹ For example, payloads in geosynchronous orbit can transfer to a low orbit (for supplies, refurbishments, etc.) with or without the benefits of aerobraking. Without aerobraking, propellant must be burned in chemical rockets to slow a vehicle down to orbital-capture velocities. Most of this propellant can be eliminated if aerobraking is used, thus increasing payload capacity. Similar payload savings arise during aerocapture of probes sent to planetary bodies.

To aid the design of an aeroassisted orbital transfer vehicle (AOTV), NASA has established an Aeroassist Flight Experiment (AFE) mission² as a precursor to AOTV. A subscale AOTV candidate shape will be used for the AFE, and it will be equipped with 11 approved flight experiments, one of which is the Rarefied-Flow Aerodynamic Measurement Experiment (RAME).³ The RAME primary objective is to measure in-flight aerodynamic forces and moments in the rarefied-flow environment, including transition into the continuum flight regime. The measurements come from accelerometers, gyros, pressure sensors, and ancillary vehicle tracking from the Tracking and Data Relay Satellite System (TDRSS). During the experiment, vehicle maneuvers are planned to explore the free-molecule flow aerodynamics with attitude. Maneuvers will be performed at several altitudes during the mission, allowing for the first time an opportunity to examine the effect of gas-surface molecule accommodation on aerodynamic coefficients in a changing environment. This paper will discuss in detail the maneuvers as well as the RAME objectives, measurement capabilities, and anticipated results.

Aeroassist Flight Experiment

Objective Overview

A flight-test model of a blunt AOTV shape launched from the Shuttle Orbiter will be used to advance vehicle design technologies applicable to an aeroassisted orbital transfer mission. This model is referred to as the "Aeroassist Flight Experiment" vehicle, and its mission is to obtain flight data that address the major technology issues for the design and operation of AOTVs. Typically, aerodynamic braking maneuvers only occur in the upper regions of the atmosphere at or near geosynchronous orbit (GEO) return velocities. Thus, a test vehicle is needed to provide design environments that cannot be simulated in ground facilities and to obtain critical aerodynamic and aerothermodynamic data to validate the computational fluid dynamic computer codes that will be used for optimal flight control system and thermal protection system design.

Vehicle Description

Figure 1 is an exploded view of the components of the AFE spacecraft along with its

cradle in the Orbiter payload bay. The aerobrake is a raked elliptical cone shape with a cone half angle of 60° and a rake angle of 73°, providing a blunt lifting body. Connected to the rear of the aerobrake is the carrier which provides the basic payload structure for the AFE spacecraft. The carrier contains avionics equipment and scientific instruments located on the interior sides of its hexagonal structure. Also included on the vehicle are thrusters and liquid propellant for three-axis control of the vehicle attitude. The solid rocket motor (SRM) is housed in the carrier structure. The SRM provides necessary propulsion to accelerate the AFE vehicle to GEO return velocity.

Typical Mission Profile

In the typical AFE mission, the AFE spacecraft is deployed from the Orbiter by the remote manipulator system (RMS) and propelled by a solid rocket motor (SRM) into the Earth's atmosphere. After an atmospheric pass, the spacecraft returns to orbital altitude and performs several rendezvous maneuvers with the Orbiter. The AFE spacecraft is heavily instrumented, and after the pass through the atmosphere and before Orbiter retrieval, recorded data will be telemetered by TDRSS. After retrieval by the Orbiter, the AFE spacecraft will be stowed and returned to Earth in the Orbiter's payload bay (Fig. 1) so that the vehicle and equipment can be further evaluated.

Trajectory Parameters

The AFE spacecraft velocity and altitude have been estimated using a nominal spacecraft entry weight of 4100 lb in a trajectory program⁴ using the 1962 U. S. Standard Atmosphere.⁵ The results of the simulation are shown in Fig. 2. One orbit after deployment, the SRM ignites at the Shuttle altitude to lower perigee and increase velocity to about 32,000 ft/sec, simulating a return from geosynchronous orbit. After the SRM burn, the velocity increases slightly as the spacecraft approaches the new perigee and then quickly decreases because of atmospheric drag. The velocity inflection point corresponding to maximum deceleration is shown. Thereafter, the velocity continues to decrease more slowly up to apogee. At this time, maneuvers are performed to rendezvous with the Shuttle Orbiter. These maneuvers occur beyond the time shown in Fig. 2. This figure summarizes the AFE mission flight mechanics and imbedded aerobraking principles. Namely, a velocity increment of about 8000 ft/sec is added to the spacecraft and subsequently removed by the atmosphere at the expense of an altitude excursion and time.

Atmosphere Parameters

Key atmosphere parameters used in the design of rarefied-flow aerodynamic measurement experiments are free-stream density and the rarefaction parameter, Knudsen number (Kn). Knudsen number is the ratio of the atmosphere mean-free-path to the spacecraft reference length. Figure 3 shows altitude profiles of these quantities based upon the 1962 standard atmosphere. Knudsen number is calculated using a reference length of 14 ft, the approximate

maximum diameter of the AFE aerobrake. For large velocities, Kn is a useful quantity, since it is one of several reliable guides to the location of the various rarefied-flow regimes. For example, the AFE spacecraft is expected to reside in the rarefied-flow transition from free-molecule flow (above about 750,000 ft) to hypersonic continuum flow (below about 250,000 ft) corresponding to Kn of 100 to 0.001, as shown in Fig. 3. Of course, the boundaries are not abrupt. That is, some gas-gas molecule interactions will occur above 750,000 ft, while below 250,000 ft, shear effects are not completely zero. However, the aerodynamic coefficients are fully expected to undergo a dramatic change in this region, and a successful rarefied-flow aerodynamic force flight experiment must be prepared to make measurements during this portion of flight. Density, of course, is important in predicting the magnitude of these aerodynamic forces.

Aerodynamic Measurements

Rarefied-Flow Aerodynamic Predictions

The determination of the aerodynamic behavior of the AFE spacecraft in the rarefied-flow regime is the RAME measurement objective. However, to define the experiment equipment, operating ranges, etc., requires some estimate of the anticipated aerodynamic behavior in this regime. To date, prediction of the aerodynamics in this regime relies heavily upon flow-field computation tools. Most notable is the direct simulation Monte Carlo (DSMC) method⁶ in the near free-molecule flow portion of the rarefied regime and nonequilibrium viscous codes⁷ near the hypersonic continuum end of this regime. Empirical "bridging" formulas based upon a variety of past flight data and ground research test data are also used. References 8 through 16 are a collection of some of the research efforts which address the rarefied-flow aerodynamic coefficients applicable to the AFE vehicle.

Force Coefficients

Bridging formulas provide a smooth blend for the aerodynamic coefficients in the region between the free-molecule flow and continuum flow. The RAME design studies use an approximate empirical bridging formula to generate the aerodynamic coefficients in this transitional flight regime. This bridging formula, which is essentially a normalized aerodynamic coefficient, is given as

$$\bar{C} = \sin^n \omega \quad 0.001 \leq Kn \leq 100$$

where

$$n = (7 - \log_{10} Kn)/5$$

and

$$\omega = \pi (3 + \log_{10} Kn)/10$$

Fig. 4 shows the functional behavior of this bridging formula between free-molecule flow ($Kn >$

100) and hypersonic continuum ($Kn < 0.001$) where $\log_{10} Kn$ is the independent variable. Also shown in the figure is a comparison between the above formula and results generated from a three-dimensional (3-D) direct simulation Monte Carlo (DSMC) technique¹³ for the AFE spacecraft at an angle of attack (α) of 17° and a sideslip angle (β) of 0° . Both lift and drag simulation results are shown in terms of normalized coefficients. The normalized coefficient, by definition, is

$$\bar{C}_i = \frac{C_{iF} - C_{iC}}{C_{iF} - C_{iC}}$$

where i = lift or drag, and subscripts C and F refer to the continuum and free-molecule values, respectively (i.e., the boundaries of the rarefied transition regime).

At the free-molecule boundary, (i.e., $\bar{C} = 1.0$ in Fig. 4), slight differences between the bridging formula and the simulation indicate that DSMC predicts free-molecule flow at Kn larger than 100. Further, using a single formula for both coefficients limits an accurate description because shear effects are not necessarily distributed equally into each component. Finally, the formula provides no wind angle provisions. Figure 5 displays a further comparison of the properly scaled force coefficients to illustrate the bridging formula limitations for the AFE application. Shown, also, are the hypersonic continuum wind-tunnel prediction values¹⁶ and the results¹² from separate free-molecule-flow calculations.

Moment Coefficients

Figure 6 shows the prediction of the pitching-moment coefficient, C_m , of the AFE vehicle in the rarefied-flow regime (dashed curve) as a function of the Kn . The sign convention and moment center are shown by the insert sketch of the AFE (shown inverted). The moment coefficient shown is generated about the nominal location of the center of gravity (c.g.) for the actual vehicle. This c.g. location is slightly offset (about 0.35 in. above the longitudinal axis) from the geometric figure such that the vehicle trims at an angle of attack of 17° in the hypersonic continuum. Figure 6 shows that for $Kn < 0.001$, C_m is approximately 0. The value of C_m is slightly higher (about 0.055) in the free-molecule flow regime assuming completely diffuse surface reflection. The intermediate Kn range (i.e., $0.001 < Kn < 100$) of C_m is approximated using the previously discussed bridging formula.

For fixed angle of attack, there is a small change in the magnitude of C_m in the rarefied-flow transition region. However, the vehicle trim angle of attack experiences a relatively large change, about 47° , principally because of changes in the location of the aerodynamic center relative to the c.g. as the flow about the vehicle changes from continuum to free-molecule flow (i.e., moving left to right in Fig. 6). In free-molecule flow, under diffuse surface reflection assumptions, the location of the aerodynamic center (or center of pressure)

forward of the c.g. produces a longitudinally unstable vehicle. Fortunately, the forces and moments are small and readily controlled. For specular surface reflection assumptions, the situation is completely different, and only small changes in trim angle should be experienced in the rarefied-flow transition regime. For Fig. 6, the trim angle shown (solid curve) has also been approximated using the aforementioned bridging formula with diffuse surface reflection conditions.

Experiment Measurement Domain

Accelerometer Range

A dedicated linear accelerometer package will be used for the RAME flight measurements. The instrument is a derivative of the High Resolution Accelerometer Package (HIRAP)¹⁷ which has successfully acquired similar rarefied-flow aerodynamic data on many Shuttle Orbiter flights.¹⁸ Figure 7 shows the results of calculations of the anticipated axial and normal channel flight deceleration levels using

$$a_i = \frac{1}{2} \rho V^2 C_i \left(\frac{S}{M} \right)$$

where i = axial or normal. The calculations include the previously mentioned trajectory, atmosphere, and aerodynamics as well as weight changes during the SRM burn and the SRM casing drop prior to the initial entry into the atmosphere. As seen in Fig. 7, the RAME instrument threshold is about 1×10^{-6} g, providing measurements on the AFE vehicle up to the free-molecule-flow region. On the outgoing portion of the atmospheric pass, the threshold is reached at about $Kn = 250$ and 700 in the normal and axial channels, respectively. For reference, the threshold of the AFE avionics accelerometers, located in the Laser Inertial Navigation System (LINS), is also shown on the figure.

Pressure Transducer Range

A pressure transducer with a range of 0 to 0.01 psia (0 to 68.95 N/m^2) will be used in the rarefied-flow aerodynamic investigation. This transducer is connected to an orifice located near the AFE vehicle stagnation point. The data provide an independent measurement of the local atmosphere conditions during flight. Figure 8 shows the approximate region (in terms of Kn) covered by the RAME pressure measurements. The P_{stag} is the expected stagnation pressure for the AFE vehicle at 17° angle of attack in rarefied flow. The curve is a combination of computational data from a 3-D viscous code, which includes chemical and nonequilibrium flow,¹⁹ in conjunction with data from a 3-D Monte Carlo simulation.¹³ Figure 8 also shows a curve of chamber pressure (labeled $P_{chamber}$) which is in the inlet tube, which connects the transducer to the outside surface. The gas in the chamber is fully thermally equilibrated, and its pressure is what the transducer will measure. An estimate of the chamber pressure was calculated based upon earlier work done for the Shuttle Orbiter nose region which includes an orifice at angle of attack on a hyperboloid.^{20, 21} The voltage

output of the transducer is connected to a 12-bit analog-to-digital converter. This provides a means to estimate the lowest pressure reading, which is shown in Fig. 8. Thus, the extent of coverage is to about $Kn = 10$, which includes most of the rarefied-flow transition regime. At larger values of Kn , pressure estimates based upon a model atmosphere which matches the flight measurements as a boundary condition will be used. For the region below $Kn = 0.02$, the instrument saturation location, pressure transducers from other experiments will operate over the rest of the hypersonic flow region.

Experiment Flight Profile

A typical RAME flight operation profile is shown in Fig. 9 in conjunction with some of the AFE major mission events and vehicle deceleration profiles. The bottom figure shows the expected deceleration levels in both the axial and normal directions. The middle figure shows in chronological order several major mission events that occur around the atmospheric pass phase of the mission. Of significance are the SRM casing jettison (annotated "drop SRM") and the location of the inbound and outbound entry interface, arbitrarily defined as 400,000 ft. Shown on the top figure are the special maneuvers to be performed during the mission to gather aerodynamic data.

Aerodynamic Maneuvers

As the vehicle exits the atmosphere, rarefied-flow aerodynamic coefficient data are obtained as a function of α and β . These data periods are labeled "Aerodynamic Maneuvers" in Fig. 9. At three altitudes (350,000, 500,000, and 650,000 ft) during the outward trajectory, a maneuver sequence is performed which includes independent sweeps of both α and β from -90° to $+90^\circ$. A fourth maneuver sequence will be executed at orbital altitudes for calibration purposes. A snapshot representation of the " α - β sweep" maneuvers for 30-deg increments is presented in Fig. 10. Each maneuver occurs at the rate of 5 deg/sec. The principal reason for obtaining samples at different altitudes is to obtain information on a major unknown in the prediction of rarefied-flow aerodynamics, namely the surface reflection/accommodation effects. Currently, a priori prediction of the rarefied-flow aerodynamics is limited because of the lack of information on gas-surface molecular interactions. The AFE offers an unprecedented opportunity to gather flight information to support surface accommodation theory development. The outbound trajectory inherently provides two major benefits to the problem: (1) the heat pulse from the atmosphere friction acts as a surface cleansing agent, and (2) the vehicle surface will be subjected to bombardment predominantly from molecular nitrogen, N_2 , at low altitudes and then, at higher altitudes, predominantly from highly reactive atomic oxygen, O. Thus, progressive changes in the aerodynamic coefficients with altitude, other than rarefaction effects, should contribute to an understanding of the behavior of surface accommodation. Figure 11 illustrates the approximate change in atmospheric composition for the major species as a function of altitude using the

1976 U. S. Standard Atmosphere model.²² Inserted are the locations of the planned maneuvers with the approximate altitude change (i.e., "maneuver window") for each maneuver sequence.

Anticipated Measurement Levels

The AFE vehicle aerodynamic force and moment coefficients have been calculated for free-molecule flow conditions.¹² These calculations were made by dividing the AFE vehicle (with the carrier afterbody) into many small flat-plate elements and then summing the elemental forces and moments over the entire body. The calculations include the extremes of surface accommodation effects, that is, diffuse and specular surface reflection. A summary of the results given in Fig. 12 clearly shows that surface accommodation assumptions have a significant impact on the coefficients.

A standardized aerodynamic acceleration parameter is used to estimate the level of acceleration expected during each α - β sweep maneuver. This parameter is defined as the acceleration when the aerodynamic coefficient is exactly 1.0. This is

$$A = \frac{1}{2} \rho V^2 \left(\frac{S}{M} \right)$$

Figure 13 presents the calculations of the standardized normal acceleration for two density models, the 1976 U. S. Standard model (solid line) and a solar minimum model (dashed line). The actual values of the AFE acceleration can be obtained using either curve with the appropriate aerodynamic coefficients. For example, using the data from Fig. 12 provides the maximum acceleration value (disregarding sign) in each of the three axes during the α - β sweep maneuvers when the AFE resides in the free-molecule flow regime. These values are shown in Fig. 13 at 500,000 and 650,000 ft. At 350,000 ft, the aerodynamic curves in Fig. 12 are modified to account for rarefied transition effects, since at this altitude, $Kn = 0.1$. This modification uses a scaling based upon the bridging formula. Clearly, the RAME sensors threshold (1×10^{-6} g) provides the required measurements capability for the selected maneuvers, including times of solar minimum.

Equipment Description

Accelerometer Package

A conceptual sketch of the RAME flight accelerometer equipment is presented in Fig. 14. The instrument is estimated to weigh about 11.5 lb, with dimensions of about 11.3 x 13.3 x 7.6 in., and to require about 17 watts of power. The basic elements of the unit consist of an orthogonal triad of pendulous accelerometer sensors (labeled "Accelerometer Assembly") and data format electronic (DFE) cards. The DFE will provide the interface between the accelerometer systems and the AFE carrier vehicle electronics systems. This interface chiefly consists of power, timing signals, and a path to store the accumulated science and housekeeping data. Internally, the unit provides 16-bit

analog-to-digital signal conversion and mode control in order to test and operate the instrument during the various stages of development, including the actual flight experiment. An alignment surface will be used to accurately align the accelerometer input axes to both the spacecraft navigation accelerometers (e.g., LINS) and the vehicle body axes. Control and data handling signals will be provided to the experiment unit through the connector assembly.

Pressure Transducer

The pressure transducer used for the RAME has a range of 0 to 0.01 psia and is the most sensitive flight sensor commercially available. Figure 15 presents a sketch of the typical cylindrical pressure transducer along with other experiment instrument components. This type of sensor has been used on a variety of NASA reentry missions, both terrestrial and planetary. The pressure is sensed by the deflection from a vacuum reference of a thin stainless steel diaphragm. The deflection (and hence pressure) is measured by electronic circuits which respond to changes in reluctance caused by the changes of the diaphragm position relative to sensing coils. The sensor weighs 3.75 lb, has cylindrical dimensions of 2.50-in. diameter and 4.68-in. height, and requires about 1.0 watt of power. The sensor is mounted on the inner side of the aeroshell and shares an inlet port with two other similar pressure sensors with higher ranges (i.e., 0.2 and 1.0 psia), not shown.

Other Instruments

The implementation of an aerodynamic flight experiment requires additional instrumentation, principally gyros and tracking data for postflight characterization of the trajectory parameters (e.g., vehicle velocity). The gyro system provides fundamental measurements used to determine aerodynamic moments, attitude information, and spurious linear accelerations due to rotational motion about the center of gravity. The AFE avionics instrument, LINS, provides changes in vehicle attitude from which angular body rates are derived. This system uses "ring-laser" gyros which resolve changes in angles to about 8.74×10^{-4} deg and has an extremely stable scale factor. The trajectory parameters will be generated separately using tracking data provided by the TDRSS in conjunction with the data from the avionics package. Data to identify thruster control activity will also be available along with the measured and monitored mass properties of the AFE vehicle.

Equipment Installation

The RAME accelerometer package is located on the AFE carrier structure as shown in Fig. 16. Included are two views of the AFE vehicle and the AFE coordinate system. The package is close to the avionics instrument system (LINS) which contains the gyros. The choice of mounting location takes into account low-frequency vibration noise and thermal gradients during the mission. After installation, location and alignment verification measurements will be performed on (1) the spatial location of the

package and (2) the alignment of the package with respect to the avionics instrument and spacecraft axes so that the flight data can be interpreted. Vehicle mass properties will be evaluated after the flight. Shown on the upper sketch in Fig. 16 is the location of the orifice for the RAME pressure transducer. At trim angle during flight (i.e., 17°), the external gas flows through a 0.1-in. orifice into about 12 in. of stainless steel tubing to the transducer mounted behind the aerobrake (not shown).

Summary

An experiment is being developed to provide measurements on aerodynamics of a blunt lifting-body vehicle in the hypersonic rarefied flow flight regime, including transition into the continuum. The experiment, called the Rarefied-Flow Aerodynamics Measurement Experiment (RAME), is part of a complement of 11 interrelated investigations which comprise the Aeroassist Flight Experiment mission. The mission is planned to be flown in 1994. The complement of experiments will address key technology issues directed toward the development and operation of aeroassisted orbital transfer vehicles. RAME will provide data in the area of aerodynamics principally for rarefied-flow aerodynamic computational code verification. The experiment includes a triaxial accelerometer package with a resolution of 1×10^{-6} g, a 0.01-psia stagnation pressure transducer, and a rate gyro system which is part of the vehicle avionics package. Other elements of the experiment (e.g., mass, thruster events, etc.) come from various AFE engineering subsystems. The design of the experiment includes aerodynamic maneuvers performed over a range of angles of attack and sideslip at several altitudes (about 350,000, 500,000, and 650,000 ft) in the rarefied-flow regime. These maneuvers will allow measurements of the vehicle aerodynamics under a variety of flow conditions and thereby provide information on the effects of surface accommodation on aerodynamic coefficients. Sensor requirements are based upon studies of the predicted behavior of the vehicle in the rarefied-flow environment. After the flight, comparisons will be made between the experimental and predicted data bases.

Acknowledgments

The author wishes to express his appreciation to J. Ritter, Lockheed Engineering & Sciences Corporation, Hampton, Virginia for his contributions and many helpful suggestions in the development of the experiment.

References

¹Walberg, G. D., "A Survey of Aeroassisted Orbit Transfer," Journal of Spacecraft and Rockets, Vol. 22, No. 1, January-February 1985, pp. 3-18.

²Jones, J. J., "The Rationale for an Aeroassist Flight Experiment," AIAA Paper 87-1508, June 1987.

³Blanchard, R. C., "Rarefied-Flow Aerodynamics Measurement Experiment on the Aeroassist Flight Experiment," AIAA Paper 89-0636, January 1989.

⁴French, R. A., MSFC, Science and Engineering Directorate, private communication.

⁵U. S. Standard Atmosphere, 1962, NASA, USAF, USWB, December 1962.

⁶Bird, G. A., "Low Density Aerothermodynamics," AIAA Paper 85-0994, June 1985.

⁷Gnoffo, P.A., "A Code Calibration Program in Support of the Aeroassist Flight Experiment," AIAA Paper 89-1673, June 1989.

⁸Hurbut, F. C. and Sherman, F. S., "Application of the Nocilla Wall Reflection Model to Free-Molecule Kinetic Theory," The Physics of Fluids, Vol. 11, No. 3, March 1978, pp. 79-96.

⁹Potter, J. L., "Transitional, Hypervelocity Aerodynamic Simulation and Scaling," Progress in Astronautics and Aeronautics: Thermophysical Aspects of Re-entry Flows, edited by J. N. Moss and C. D. Scott, Vol. 103, 1986, pp. 79-96.

¹⁰Blanchard, R. C. and Walberg, G. D., "Determination of the Hypersonic-Continuum/Rarefied-Flow Drag Coefficient of the Viking Lander Capsule I Aeroshell from Flight Data," NASA TP 1793, December 1980.

¹¹Dogra, V. K., Moss, J. N., and Simmonds, A. L., "Direct Simulation of Aerothermal Loads for an Aeroassist Flight Experiment Vehicle," AIAA Paper 87-1546, June 1987.

¹²Blanchard, R. C. and Hinson, E. W., "Free Molecule Flow Force and Moment Coefficients of the Aeroassist Flight Experiment Vehicle," NASA TM 101600, July 1989.

¹³Celenligil, M. C., Moss, J. N., and Blanchard, R. C., "Three Dimensional Flow Simulation About the AFE Vehicle in the Transitional Regime," AIAA Paper 89-0245, January 1989.

¹⁴Kotov, V. M., Lychkin, E. N., Reshetin, A. G., and Schelkonogov, A. N., "An Approximate Method of Aerodynamic Calculation of Complex Shape Bodies in a Transition Region," 13th International Symposium of Rarefied Gas Dynamics, Vol. 1, 1982, pp. 487-494.

¹⁵Koppenwallner, G., "The Drag of Simple Shaped Bodies in the Rarefied Hypersonic Flow Regime," AIAA Paper 85-0998, June 1985.

¹⁶Wells, W. L., "Measured and Predicted Aerodynamic Coefficients and Shock Shapes for the Aeroassist Flight Experiment (AFE) Configuration," NASA TP-2956, January 1990.

¹⁷Blanchard, R. C. and Rutherford, J. F., "Shuttle Orbiter High Resolution Accelerometer Package Experiment: Preliminary Flight Results," Journal of Spacecraft and Rockets, Vol. 22, No. 4, July-August 1985, p. 474.

¹⁸Blanchard, R. C., "Rarefied Flow Lift-to-Drag Measurements of the Shuttle Orbiter," 15th Congress of International Council of Aeronautical Sciences (ICAS), Paper No. ICAS-86-2.10.2, September 1986.

¹⁹Gnoffo, P. A., private communication.

²⁰Bienkowski, G. K., "Interference of Free Stream Properties from Shuttle Upper Atmosphere Mass Spectrometer (SUMS) Experiment," *Rarefied Gas Dynamics*, Vol. 1, Proceedings of the 14th International Symposium, edited by Hakuro Oguchi, 1984, pp. 295-302.

²¹Moss, J. N. and Bird, G. A., "Monte Carlo Simulations in Support of the Shuttle Upper Atmospheric Mass Spectrometer Experiment," AIAA Paper No. 85-0968, June 1985.

²²U. S. Standard Atmosphere, 1976, NOAA, NASA, USAF, October 1976.

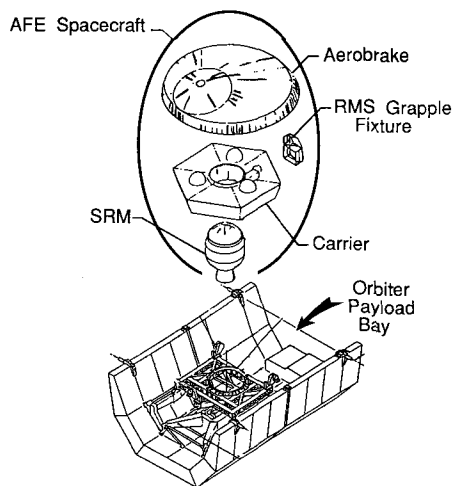


Fig. 1 Aeroassist Flight Experiment components and cradle in Orbiter payload bay.

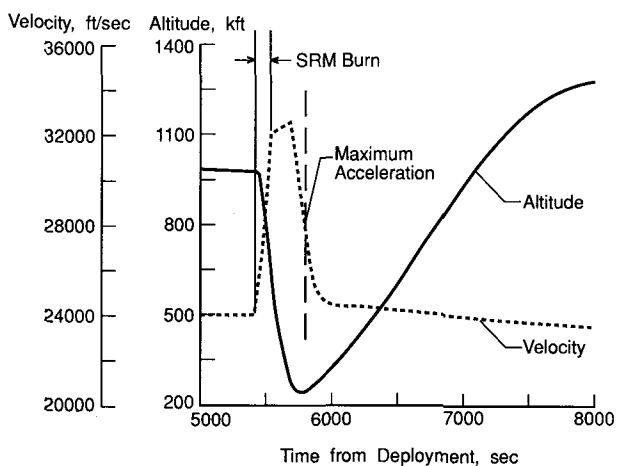


Fig. 2 Typical AFE altitude and velocity time history.

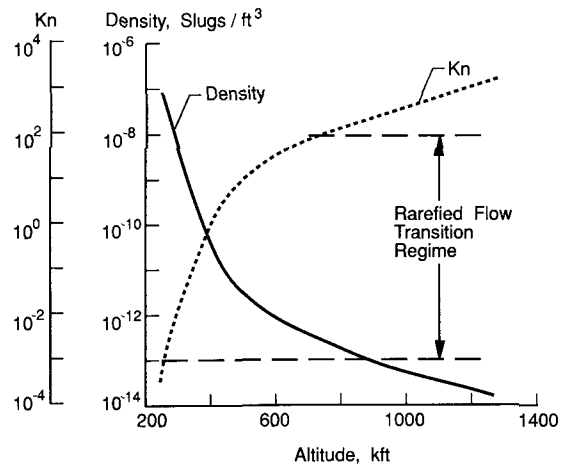


Fig. 3 Density and Knudsen Number profiles.

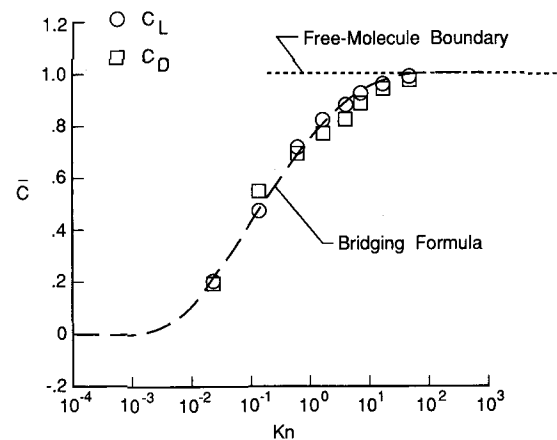


Fig. 4 Comparison of bridging formula with 3-D Monte Carlo simulation, $\alpha = 17^\circ$, (ref. 13).

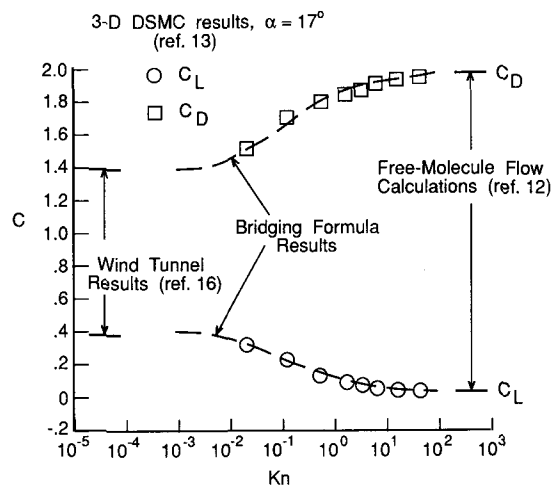


Fig. 5 Comparison of bridging formula with C_L and C_D .

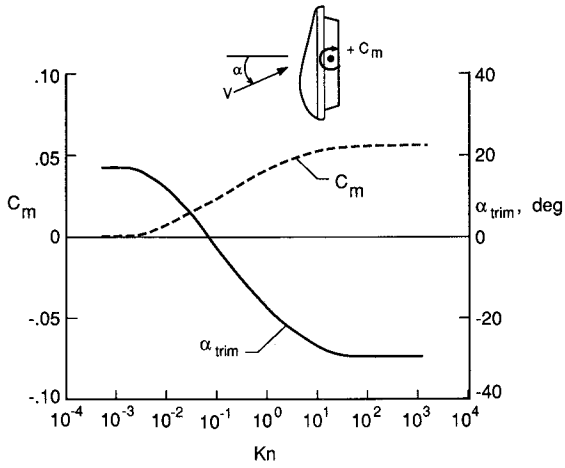


Fig. 6 Predicted AFE pitching-moment coefficient for $\alpha = 17^\circ$ and pitch trim angle of attack throughout the rarefied flow regime.

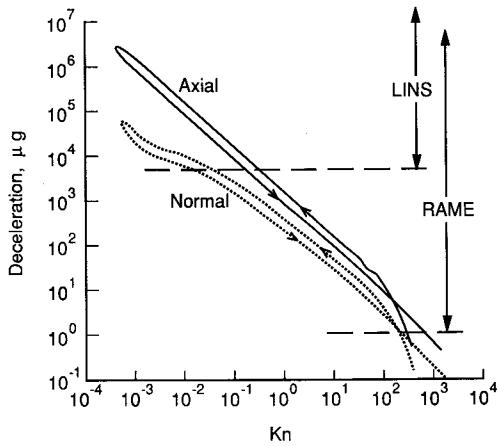


Fig. 7 RAME and AFE avionics accelerometer (LINS) measurement ranges.

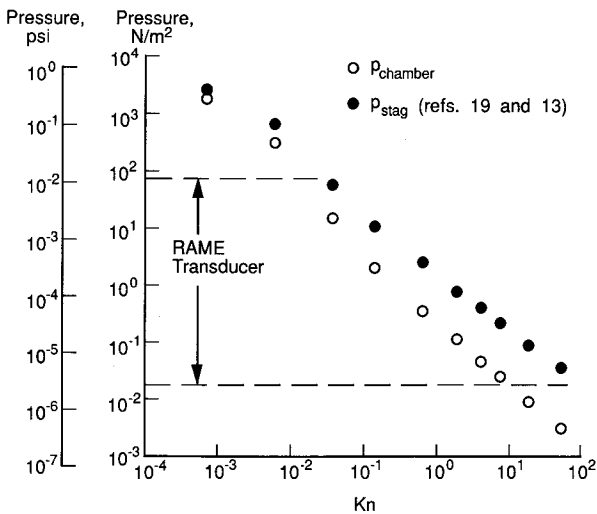


Fig. 8 Approximate RAME stagnation pressure transducer range.

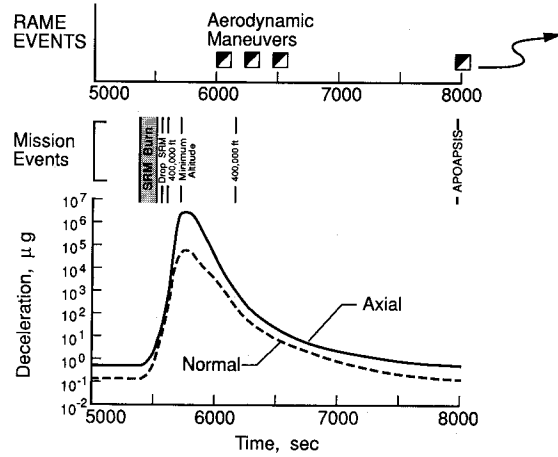


Fig. 9 Typical RAME flight operations profile.

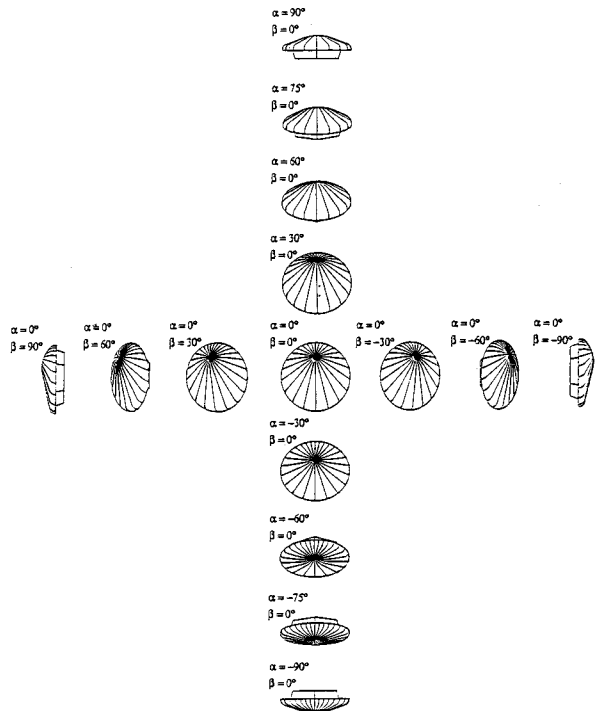


Fig. 10 Orientation of AFE during the RAME " $\alpha - \beta$ sweep" maneuver (velocity vector directed toward viewer).

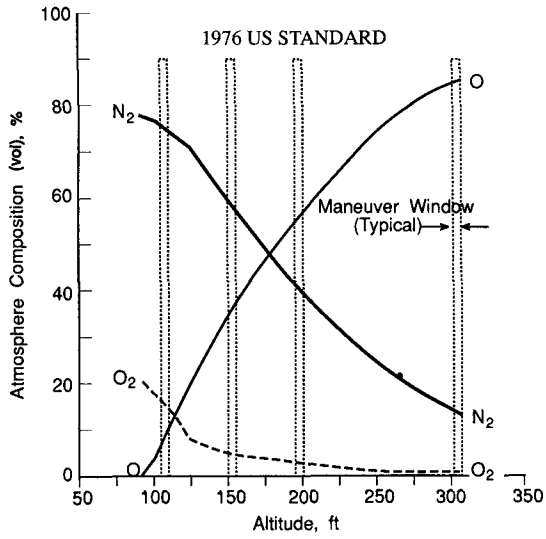


Fig. 11 Environment during RAME aerodynamic maneuvers.

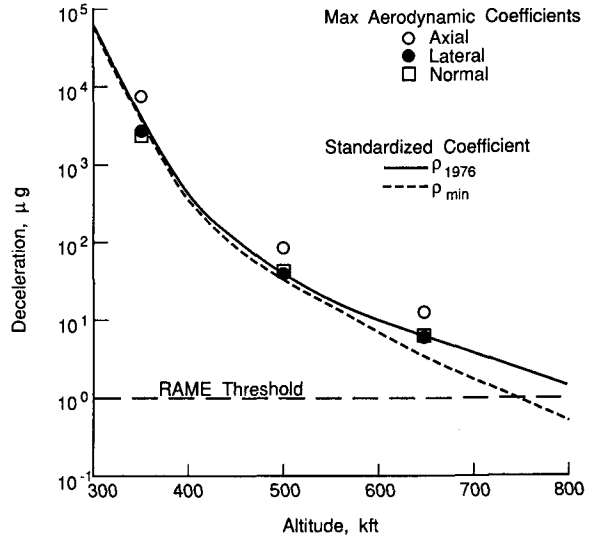


Fig. 13 Approximate acceleration levels during the RAME " $\alpha - \beta$ sweep" maneuvers.

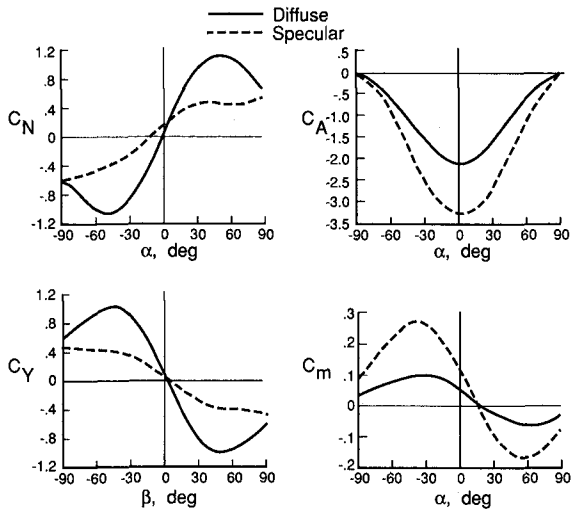


Fig. 12 AFE free-molecule flow aerodynamics for diffuse and specular surface reflection, $s = 11.25$, $T_W/T_\infty = 0.224$, (ref. 12).

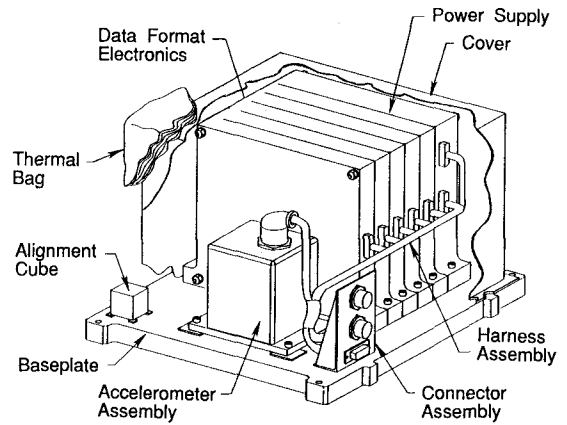


Fig. 14 Conceptual RAME accelerometer package.

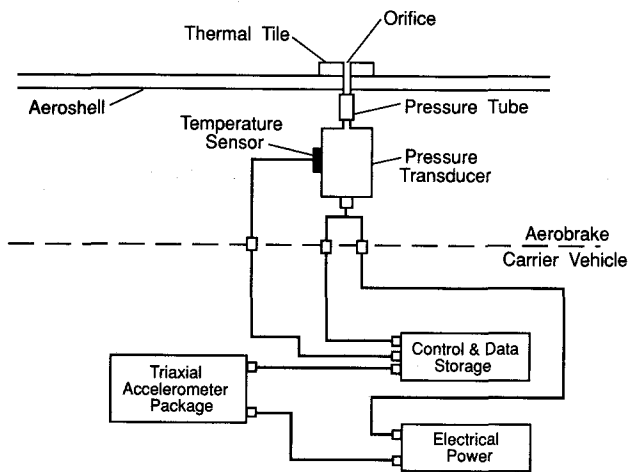


Fig. 15 Block diagram of RAME pressure transducer with other components.

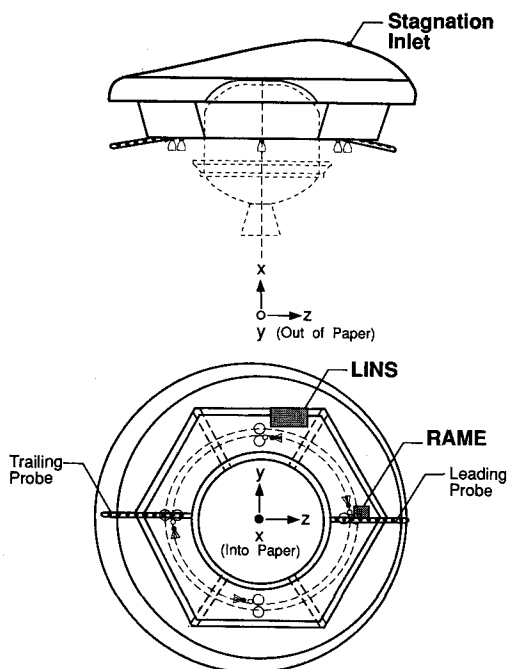


Fig. 16 Approximate location of RAME equipment on AFE vehicle.

Copyright © 1990 by the American Institute of Aeronautics and Astronautics, Inc. No copyright is asserted in the United States under Title 17, U.S. Code. The U.S. Government has a royalty-free license to exercise all rights under the copyright claimed herein for Governmental purposes. All other rights are reserved by the copyright owner.